# Skin Harvesting Robotization with Force Control

G. Duchemin, E. Dombre, F. Pierrot, Ph. Poignet
LIRMM – UMR 5506 CNRS / Université Montpellier II
161 rue Ada, 34392 Montpellier Cedex 5, France
Corresponding author: duchemin@lirmm.fr, Phone: (33) 4 67 41 85 65, Fax: (33) 4 67 41 85 00

## Abstract

*This paper presents a new research program in robotized reconstructive surgery for skin harvesting with a mechanical device under force control. In a first part, we present the problem of robotizing skin harvesting in terms of medical and robotic constraints. Then, we describe the system and force control law implemented. Some experiments on rubber foam are presented and finally, emphasis is put on safety issues.*

## 1. Introduction

During the last twenty years, new robotic applications have come up in non-manufacturing areas, especially in medical domain. Many developments of robotic systems to assist surgeons have been achieved, providing impressive results, especially in neurosurgery, laparoscopy and orthopedic surgery. The general methodology of Computer Assisted Medical Intervention (CAMI) is based on the classical "perception-simulation/planning-action" loop [1]; the perception phase corresponds to data acquisition provided by pre-operative or intra-operative medical images; the simulation/planning phase is a definition of the operative strategy adopted by analysis and matching of the different medical data; the action phase is the effective realization of the operation involving an assistance device such a robot. Referring to [2], robotic systems dedicated to action involved in medical applications can be sorted in three classes: passive arms, that have no actuator and no autonomy [3]; active systems performing planned operations by themselves since all joints are actuated (laparoscopy [4], orthopedic surgery with the parallel robot CRIGOS [5] or with the serial robot ROBODOC for total hip replacement [6], neurosurgery with Minerva [7], prostatectomy [8], or maxillofacial surgery [9]); and, at last, semi-active systems for which power is cut-off during critical phases of the tasks and actuators are not directly used to guide the robot, but rather to help doctor to guide and handle his tools (in neurosurgery with the Neuromate [10], or with the Neurobot [11], or for total knee replacement surgery [12]). Recently, three other categories have been added to the precedent classification: synergistic systems which are roughly programmable semi-active systems and are able to limit dynamically the surgeon gesture (different prototypes like PADyC for pericardic puncture, Cobot used for knee surgery, or ACRobot [13]); tele-robotic systems allowing remote interventions [14]; and finally, micro-robotic systems, like Micro Electrical Mechanical Systems (MEMS) for endo-corporeal surgery [15].

This paper deals with a new robotized medical application for reconstructive surgery with a dedicated force controlled active arm.

Skin harvesting on human body in order to graft or to culture the sample requires a high accuracy in the gesture and is physically very demanding for the surgeon due to the efforts he has to exert: indeed, it aims at harvesting a constant thickness strip of skin (few tenths of millimeter) with a "shaver-like" device called dermatome (Figure 1). Besides, it requires a long period of training and has to be practiced regularly (for orthopedic physicians for instance, this gesture is not completely mastered since it may not be a daily operation). According to the burn degree, skin strips may be harvested on different locations on the patient: thighs, buttocks, head (thus, scars are hidden by hair), under sole or armpit.

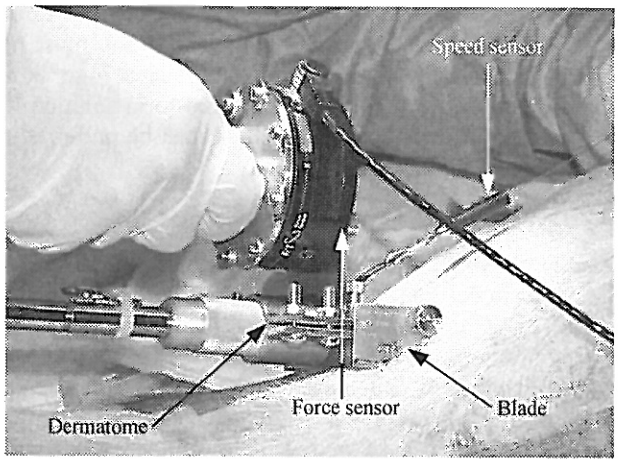


**Figure 1.** *Surgeon performing skin harvesting on a pig*

A dermatome is a simple mechanical device offering only two adjustable parameters: the blade speed which is modified thanks to a pedal, and the maximum cutting depth which is selected on the dermatome head. This depth selection does not guarantee at all the actual cutting depth: depending on the user skill, for a given depth selection, the resulting skin strip thinness may range from the selected depth, down to zero.

In the frame of this ambitious project[1], we will embed part of a specialized surgeon skill in a robotic system called SCALPP (as "Système de Coupe Automatisé pour Le Prélèvement de Peau"), in order to bring this skill to other surgeons who do not practice harvesting as a routine.

## 2. Problem Statement

We describe in this section the medical and robotic requirements to robotize skin harvesting which lead us to design SCALPP (the prototype robot has been manufactured by the SINTERS company[2]).

Since the robot aims at being used in an Operating Room (OR), the system (arm and controller) must be quickly and easily moved by a single person. Then, it must be mounted on wheels and as light as possible. Moreover, the robot position in the OR must take into account the various medical instruments (anaesthetic pipes, electrocardiogram...) and surgeon workspaces. In emergency case, the system must be quickly released from the patient body, without risk for him, neither for the medical staff nor for the equipment. For asepsis requirements, no non-medical equipment must be closer than 400 mm from the operating table.

During a feasibility study (see [16] and Figure 1), we demonstrated that force involved in the process may reach up to 100 N and that harvesting velocity is lower than 5 $cm.s^{-1}$. Such a force means that the driving motors should be quite bulky, especially on the wrist. For obvious safety reasons, during the harvesting motion, the arm must not cross a singularity configuration or reach a joint limit. Finally, for accuracy constraints, closed-form solution for the Inverse Geometric Model (IGM) must be preferred to a polynomial or numerical method.

## 3. SCALPP Robotic System

All the above-mentioned medical and robotic constraints forced us to design a convenient architecture [17]. Firstly, we selected and dimensioned the shoulder: a SCARA carrier has been chosen owing to its cylindrical workspace and the facility to compensate for gravity effect even in case of power breakdown. Secondly, a suitable wrist has been proposed: we showed that the non-spherical wrist presented in Figure 2 fulfilled the four main constraints, namely: absence of singularity in the workspace, closed-form solution for the IGM, motors taking up little space and sufficient joint position range. In order to allow force control, a Force/Torque (F/T) sensor is integrated in the wrist. The dermatome is fixed to the tip of the arm.

This 6-axes arm is fixed to a mobile support mounted on wheels (Figure 3), which contains four racks: an industrial PC running the Real Time and Multitasking Operating System QNX for the high level control, a power supply unit, a logical unit formatting the I/O signals and a rack including the resolvers and translator boards for the stepper motors.

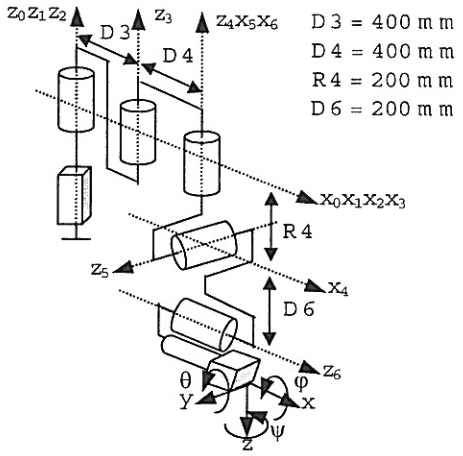


**Figure 2.** *Architecture of the SCALPP arm*

**Figure 3.** *SCALPP system*

The User Interface (UI) – a console desk with a LCD screen – has been developed in close cooperation with the surgeons in order to provide user-friendly tools to handle the system. Four modes are allowed: a `teaching` (or `manual`) mode and an `automatic` mode dictated by the process constraints; a `reconfiguration` mode to comply with the arm architecture; and a `free` mode for safety reasons.

During the `teaching` mode, the surgeon teaches to the robot the initial and final poses, ${}^0P^I$ and ${}^0P^J$ on the patient's skin: the robot is totally compliant in this mode since the desired forces are set to 0 and the user moves it by grabbing the dermatome handle. As soon as two poses

[1] This work has been supported partly by funds from "Ministère de l'Education Nationale et de la Recherche" and "Région Languedoc-Roussillon".

[2] SINTERS SA, BP 1311, Parc Technologique Basso Cambo, 5 rue Paul Mesplé, 31106 Toulouse Cedex 1, France.

are recorded on the skin and a desired force $F_z^d$ is selected by the surgeon with the UI, the `automatic` mode is switched on. Harvesting begins when the DMS pedal is pressed. The seven steps of automatic motion are described on Figure 4.

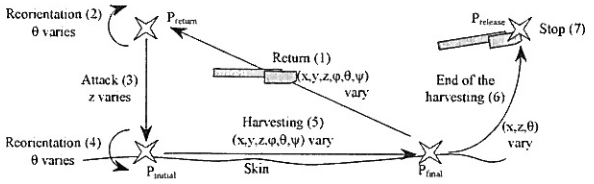


**Figure 4.** *Different steps of motion in* `automatic` *mode*

The `free` mode is activated by the user for moving the arm without any force control: in this mode, the axes are not driven, and any motion inside the joint limits can be performed thanks to the arm reversibility. This mode is used to release the arm from the patient body in emergency case for example, or to place the arm in a specific position (parking position for instance).

At last, the `reconfiguration` mode is used to pass through the only remaining arm singularity position (the "classical" elbow singularity of the SCARA robot when $q_3$=0°).

## 4. Force control

Force control schemes have been widely addressed in the literature [18]. An usual classification consists in dividing force control scheme into two families: passive compliance and active compliance (and sometimes mix compliance). The first one uses a deformable structure mounted at the arm tip without force measurement. In the second one the robot behavior is adapted according to the contact forces; there are three classes of active compliance control: without force measurement (for instance, impedance control [19]); with force measurement but without desired force, like explicit force-feedback control (stiffness and damping controls [20]); with force measurement and control (active stiffness, hybrid [21] and external [22] controls).

Since the application requires force control to move the arm in the `teaching` and `automatic` modes, we discarded all controls without F/T sensor. Among the remaining controls, active stiffness and hybrid controls have been also discarded: indeed, the first one uses the Jacobian matrix, which may induce instability near singularity configurations; the second one selects the directions which must be force controlled and the direction which must be position controlled. The external control (called also nested or cascade structure) is the only force control suited for our application. Here again, different schemes can be proposed depending on the space where the summation of force and position components is achieved (joint or Cartesian summation) and on the position control (joint control by IGM or Jacobian matrix and Cartesian control). External control with Cartesian summation and joint control by IGM has been chosen in order to avoid use of Jacobian matrix, which could induce numerical problems. To summarize, the key advantages of external control are the following [22]: the joint position loop is always activated, providing stability and avoiding switching between the position servo loop and the force loop; it works very well with very simple and reliable (thus safe) control laws (like a PID at the joint level and a I for the external force loop); it is easy to implement on any kind of controller; the robot will not move, unless an effort is applied on the dermatome (below the force sensor); at last, it allows designing the control software in an incremental manner, facilitating the tuning of the parameters and the validation process (joint control, Cartesian space control and force control loop).

## 5. Implementation of an external force control scheme

We detail here the implementation of the external force control scheme on SCALPP (Figure 5). In this figure, two parts appear clearly: the force control loop and the transformation from the Cartesian space to the joint space. A third function concerns the low level joint control carried out by an eight-axes board, which controls the six stepper motors of the arm.

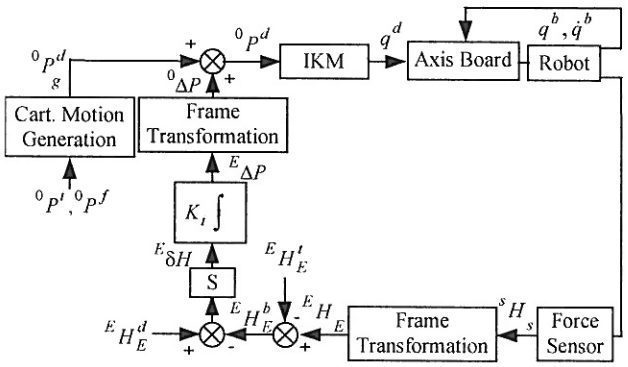


**Figure 5.** *External force control scheme*

The tool center point position is defined by the Cartesian coordinates and we use a roll-pitch-yaw description for the orientations. The linear motion of the origin of the tool frame from an initial pose ${}^0P^i$ to a final pose ${}^0P^f$ is given by:

$$ {}^0P_g^d(t) = {}^0P^i + r(t)\left({}^0P^f - {}^0P^i\right) \qquad (1) $$

In order to assure velocity and acceleration continuities, a five degree interpolation polynomial is used for r(t). In the `teaching` mode, the motion generation is not enable whereas during the `automatic` mode, the initial pose

${}^0P^i$ and final pose ${}^0P^f$ are those which have been taught to the arm by the surgeon during the `manual` mode.

The 6-axes F/T sensor at the arm tip allows to measure the force exerted by the environment on the arm. The forces are measured in the sensor frame $R_s$ and are noted ${}^sH_s = \left[{}^sF_s^T \; {}^sM_s^T\right]^T$. However, in order to control the arm, the force vector ${}^EH_E = \left[{}^EF_E^T \; {}^EM_E^T\right]^T$ must be known in the tool frame $R_E$ and is noted:

$$\begin{cases} {}^EF_E = -{}^sA_E^T \, {}^sF_s \\ {}^EM_E = -{}^sA_E^T \left({}^sF_s \times {}^sX_E + {}^sM_s\right) \end{cases} \quad (2)$$

where the transformation matrix between $R_s$ and $R_E$ is given by ${}^sT_E = \begin{bmatrix} {}^sA_E & {}^sX_E \\ 0_{1\times3} & 1 \end{bmatrix}$. The minus sign in (2) represents effort exerted by the tool on the environment.

Finally, the feedback force ${}^EH_E^b$ is given by:

$$\begin{cases} {}^EF_E^b = {}^EF_E - {}^EF_E^t \\ {}^EM_E^b = {}^EM_E - {}^EM_E^t \end{cases} \quad (3)$$

where ${}^EH_E^t = \left[{}^EF_E^{t\,T} \; {}^EM_E^{t\,T}\right]^T$ stands for the force vector of the tool gravity compensation.

Knowing the desired force ${}^EH_E^d$ and the feedback force ${}^EH_E^b$, both expressed in the tool frame, the force error ${}^E\delta H$ can be computed at any time:

$${}^E\delta H = S\left({}^EH_E^d - {}^EH_E^b\right) \quad (4)$$

where S is the diagonal selection matrix, composed of 1 and 0, and allowing to select the force control directions. For instance, during the `teaching` mode, all axes are force controlled, meaning that $S = Id_6$ and ${}^EH_E^d = 0_{6\times1}$, whereas during the `automatic` mode $S = diag[0\ 0\ 1\ 1\ 1\ 0]$ and ${}^EH_E^d = \left[0\ 0\ F_z^d\ M_x^d\ M_y^d\ 0\right]^T$, since only force along z ( $F_z^d$ is selected by the surgeon), and momenta about x and y are controlled.

Thanks to the force error vector ${}^E\delta H$ an increment ${}^0\Delta P$ expressed in the base frame $R_0$ can be computed, in order to change the desired pose vector ${}^0P_g^d$ coming from the motion generation and expressed in the base frame $R_0$. A previous study [23] shown that an integral law was the most appropriate for the command:

$${}^E\Delta P = K_i \int {}^E\delta H dt \quad (5)$$

where $K_i$ represents the integral gain.

Using a frame transformation computed with the Direct Geometric Model ${}^0P^d = f\left(q^d\right)$, it is possible to know the situation ${}^0\Delta P$ expressed in the base frame. Finally, we have:

$${}^0P^d = {}^0P_g^d + {}^0\Delta P \quad (6)$$

The closed-form solution of the IGM provides the joint positions sent to the axes board.

# 6. Experimental Results

External force control is usually used on rigid surfaces, contrary to the harvesting process where the surface is a soft tissue. To simulate skin, foam rubber coated with silicon is used. In the two following experiments the desired $F_z^d$ value is set to 60 N.

The first experiment (Figure 6) is performed on a planar surface: the left graph represents the evolution of ${}^0P_{gz}^b$ and ${}^0P_z^b$.

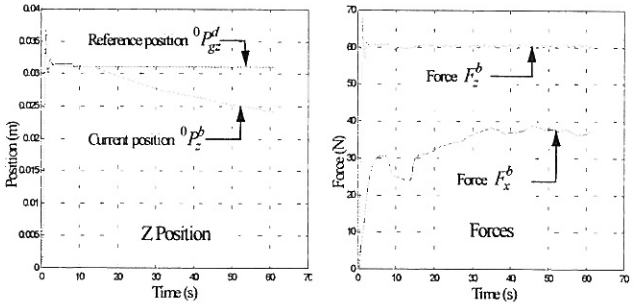


**Figure 6.** *Harvesting on a plane surface*

The difference between both curves is obviously due to the ${}^0\Delta P$ term coming from the force control law (6). The right graph shows the force evolutions, in two directions x and z: $F_z^b$ remains constant all over the path and it is worth noting that the force $F_x^b$ is quite large (about 35 N), contrary to a rigid surface. The sudden variation at 15 sec. is due to the reorientation of the tool (phase 4). In fact, during the motion, due to the flexibility of the foam rubber, a bump is developing ahead the dermatome.

In order to follow non planar surfaces such as a head or buttocks with a good accuracy, we added a laser telemeter at the tip of the wrist (Figure 7); indeed, the torque resolution (0.015 N.m) of the F/T sensor is not good enough to control the $M_y$ torque during the harvesting. Thanks to a reference measure $d_{ref}$ acquired before the motion (phase 5), the distance $d$ between the skin and the wrist can be controlled (Figure 8: left side, pitch angle evolution; right side, torque evolution); thus, we compute the $M_y^b$ torque by the obvious proportional relation:

$$M_y^b = k(d - d_{ref}) \quad (7)$$

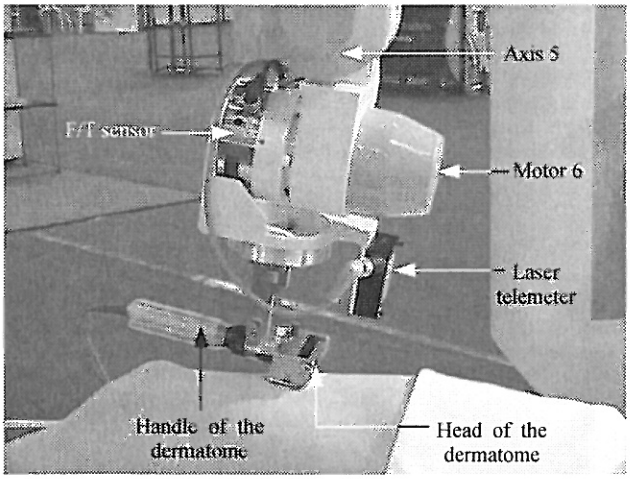


**Figure 7.** *Detail of the tip of the wrist*

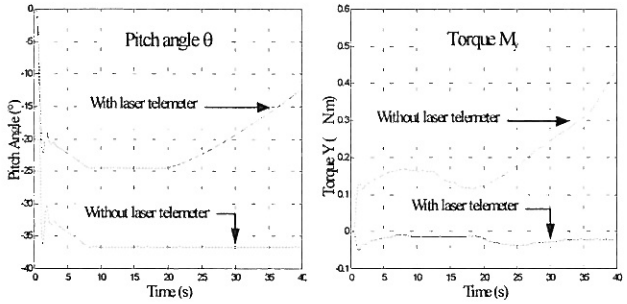


**Figure 8.** *Comparison of harvesting on a spherical surface*

Without this laser telemeter, although contact with skin is kept and force along z axis is applied, the dermatome blade isn't always in contact with the skin, since the pitch angle θ remains constant and the torque $M_y^b$ varies (Figure 9). The linear segment at 10 sec. on the curve without laser represents the fact that after the reorientation phase (phase 4), the robot waits for few seconds to stabilize the efforts before beginning the harvesting motion.

# 7. Safety Issues

## 7.1. Safety requirements for medical systems

Different constraints have to be considered when designing medical robots since they are directly in contact with human body and interact with surgeons. That's the reason why, important issue is to integrate the securities at mechanical, electrical and software levels [24], [25]. Beyond the rules enacted, the most important condition is that the robot behavior has to be controlled at any time. In fact, in case of emergency stop or failure, the robot mustn't hurt the patient or the medical staff, and should quickly come back to a position from which it can be started again. Moreover, force applied on the patient must be controlled and supervised by the surgeon at any time to avoid incident. Finally, the surgical tool has to remain in a predefined work area. We described in the following sections, the most important safety aspects we developed to make SCALPP an intrinsically safe robotic system.

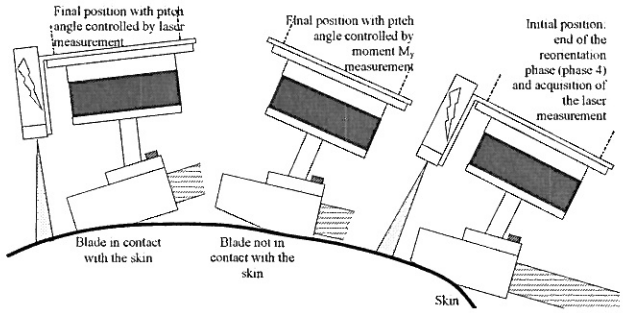


**Figure 9.** *Motion on non planar surface*

## 7.2. Mechanical Safeties

Owing to the SCARA structure, no specific brakes are required to compensate gravity (except for the first axis which is balanced thanks to a counterweight). Moreover, the mobile support is counterbalanced avoiding any risk of falling over due to the force exerted during the operation. A locking system under the support prevent it to move once the robot has been placed.

Stepper actuator technology has been selected. Indeed, a stepper motor needs pulses to rotate. If the output of a translator were stuck at a constant value, the motor shaft would receive a holding torque which prevents it rotating (contrary to the DC or AC motors which still continue to rotate).

On each joint the combination of two absolute resolvers suppresses time consuming and potentially hazardous initialisation procedures: one mounted on the motor output shaft (fine position sensing), the other mounted on the output reduction gear (coarse sensing of the joint location). To reduce output axis speed, harmonic drives have been chosen as reduction gears for their high efficiency, low backlash and flexibility.

## 7.3. Electrical Safeties

Any action on emergency button switches off immediately the arm power. Two redundant circuits have been wired on a watch-dog board in order to manage the security from a software point of view. If the high level controller is locked, the cyclic signal sent to the watch-dog is stopped, inactivating it and switching off the power. Finally, a motion of the robot in `automatic` or `teaching` modes needs an action on the DMS:

therefore, the behavior of the robot is always supervised by the surgeon.

### 7.4. Software Safeties

In addition to the mechanical and electrical securities, the high-level program has been built thanks to a software analysis based on security. The main solutions implemented are presented in this section.

We chose the multitasking OS QNX dedicated to real-time running on PC. Five processes are running sequentially, one for each specific function: security, working modes, force, I/O communications and translators controls. In addition to the watch-dog card, the dedicated security process checks the activity of the others ones. If anyone of these processes is locked, then the emergency procedure is switched on.

During the `automatic` and the `teaching` modes, an emergency procedure is switched on as soon as a tracking error is detected on a joint (difference between the current value $q_j^b$ and the desired value $q_j^d$ beyond a threshold).

In addition, to detect jamming of the dermatome blade (due for example to a bad lubrication of the mechanism), a FFT algorithm computes the resonance frequency of the blade thanks to analysis of the dermatome noise.

Finally, in case of a default or if the DMS pedal is switched off during the `automatic` mode, different phases of clearing have been planed depending on whether blade is in contact with the skin or not.

## 8. Conclusion and future works

In this paper, we have presented our methodology to robotize skin harvesting. A feasibility study and an analysis of the process has allowed us to design a force controlled robot adapted to the medical environment. A convenient force control scheme has been chosen, and appropriate safety rules have been applied to make SCALPP intrinsically safe.

In the future works, a precise analysis of the mechanical (elasticity, viscosity) properties of the skin will allow us to improve the force control law. Moreover, other experiments must be achieved on silicon and foam rubber, as well as validation on animals.

## References


[1] S. Lavallée *et al.* Image guided operating robot : a clinical application in stereotactic neurosurgery. Proc. IEEE ICRA, Nice, France, pp. 618-624, May 1992.

[2] P. Cinquin *et al.* Computer Assisted Medical Interventions. Passive and semi-active aids. IEEE Engineering in Medecine and Biology magazine, Special issue « Robots in Surgery », vol. 14, no. 3, pp. 254-263, May-June 1995.

[3] R. Mösges *et al.* CAS – Computer Assisted Surgery. An Innovative Surgical Technique in Clinical Routine. Proc. Computer Assisted Radiology 89, Berlin, Germany, pp. 413-415, H.U. Lemke Editor, Springer-Verlag, 1989.

[4] R.H. Taylor *et al.* A Telerobotic Assistant for Laparoscopic Surgery. IEEE Engineering in Medecine and Biology magazine, Special issue « Robots in Surgery », vol. 14, no. 3, pp. 279-288, May-June 1995.

[5] G. Brandt *et al.* A Compact Robot for Image Guided Orthopaedic Surgery. Proc. CVRMed-MRCAS'97, pp. 779-788, Lecture Notes in Computer Science Series, vol. 1205, Springer-Verlag, 1997.

[6] P. Kazanzides. Robot Assisted Surgery: the ROBODOC experience. 30th Symp. on Robotics, Tokyo, Japan, pp. 281-286, 1999.

[7] D. Glauser. Mechanical concept of the neurosurgical robot 'Minerva'. Robotica, vol. 11, pp. 567-575, 1993.

[8] B.L. Davies *et al.* Prostatic resection : an exemple of safe robotic surgery. Robotica, vol. 11, pp. 561-566, 1993.

[9] T.C. Lueth *et al.* A Surgical Robot system for Maxillofacial Surgery. IEEE Conf. on IECON, Aachen, Germany, pp. 2470-2475, September 1998.

[10] F. Badano and F. Danel. The Neuro-Skill Robot : a New Approach for Surgical Robot Development. Proc. Int. Symp. on MRCAS, Baltimore, USA, pp. 318-323, November 1995.

[11] B. Davies *et al.* Neurobot : a special-purpose robot for Neurosurgery. Proc. IEEE ICRA, San Francisco, CA, pp. 4104-4109, April 2000.

[12] T.C. Kienzle III *et al.* Total Knee Replacement. IEEE Engineering in Medecine and Biology magazine, Special issue « Robots in Surgery », vol. 14, no. 3, pp. 301-306, May-June 1995.

[13] J. Troccaz *et al.*. The Use of Localizers, Robots and Synergistic Devices in CAS. Proc. CVRMed-MRCAS'97, pp. 727-736, Lecture Notes in Computer Science Series, vol. 1205, Springer-Verlag, 1997.

[14] G.S. Guthart and J.K. Salisbury Jr. The Intuitive™ Telesurgery System : Overview and Application. Proc. IEEE ICRA, San Francisco, pp. 618-621. April 2000.

[15] M.C. Carrozza *et al.* The Development of a Microrobot System for Colonoscopy. Proc. CVRMed-MRCAS'97, pp. 779-788, Lecture Notes in Computer Science Series, vol. 1205, Springer-Verlag, 1997.

[16] F. Pierrot *et al.* Robotized reconstructive surgery : ongoing study and first results. Proc. IEEE ICRA, San Francisco, pp. 1615-1620, April 2000.

[17] G. Duchemin *et al.* SCALPP: a 6-dof robot with a non-spherical wrist for surgical applications. Proc. on ARK, Piran-Portoroz, Slovenia, pp. 165-174, June 2000.

[18] T. Yoshikawa. Force Control of Robot Manipulators. Proc. IEEE ICRA, San Francisco, CA, pp. 220-226, April 2000.

[19] N. Hogan. Impedance Control: An Approach to Manipulation: Part I – Theory, Part II – Implementation, Part III – Applications. Trans. ASME, J. of Dynamics Systems, Measurement and Control, vol. 107, pp. 1-24, March 1985.

[20] K. Salisbury. Active Stiffness Control of a Manipulator in Cartesian Coordinates. Proc. 19th IEEE Conf. on Decision and Control, Albuquerque, pp. 95-100, December 1980.

[21] A. Pujas *et al.* Hybrid position/force control : task description and control scheme determination for a real implementation. IROS'93, Yokohama, Japan, pp. 841-846, July 1993.

[22] V. Perdereau and M. Drouin. A New Scheme for Hybrid Force-Position Control. Robotica, vol. 11, pp. 453-464, 1993.

[23] E. Dégoulange *et al.* Determination of a force control law for an industrial robot in contact with a rigid environment. IEEE Conf. on Systems, Man and Cybernetics, Le Touquet, France, vol. 2, pp. 270-275, October 1993.

[24] A. Davies. Safety of medical robots. Proc. 6th ICAR, Tokyo, Japan, pp. 311-317, 1993.

[25] E. Dombre *et al.* Intrisically safe active robotic systems for medical applications. Proc. of 1st IARP/IEEE-RAS Joint Workshop on Technical Challenge for Dependable Robots in Human Environments, Seoul, Korea, May 2001.